Beam-energy dependence of the viscous damping of anisotropic flow

Niseem Magdy
Stony Brook University
For the STAR Collaboration
niseem.abdelrahman@stonybrook.edu

CPOD2017

QCD Phase Diagram

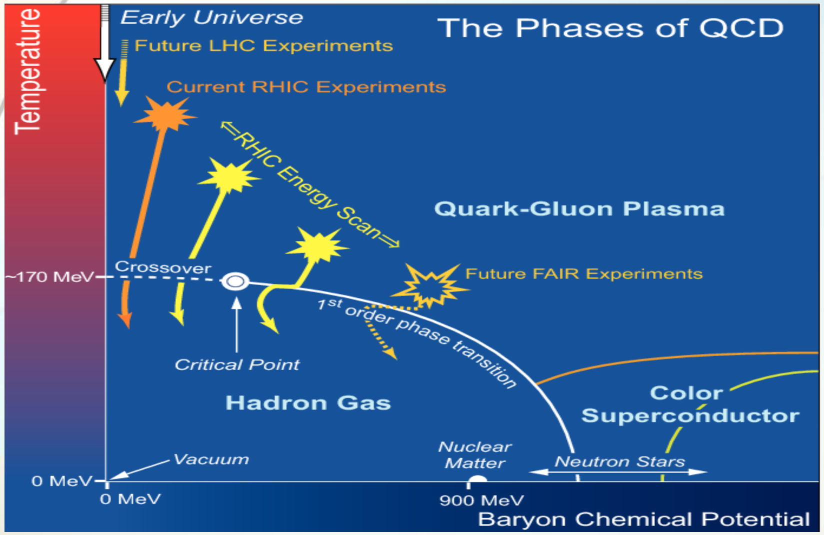

- Strong interest in the theoretical calculations which span a broad (μ_B, T) domain.

QCD Phase Diagram

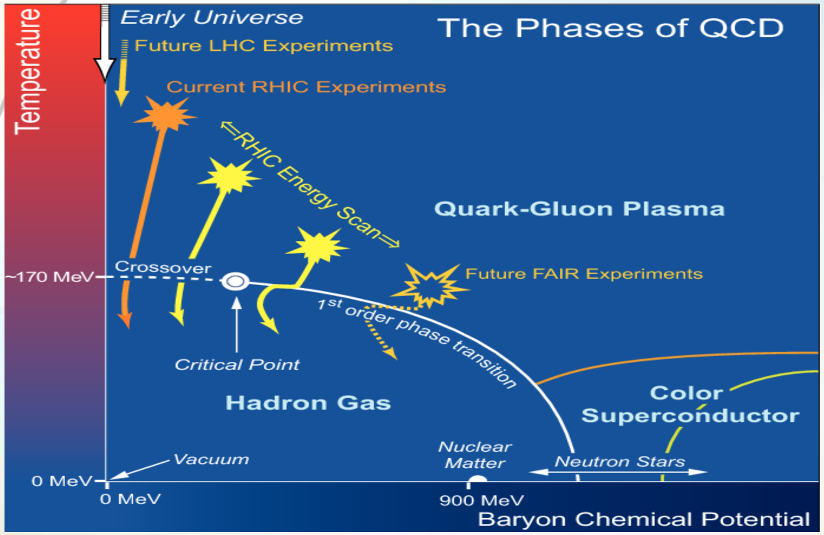

- Strong interest in the theoretical calculations which span a broad (μ_B, T) domain.

- The $^{\eta}/_{s}$ values are tuned in model calculations to describe the experimental flow data at different collision energies

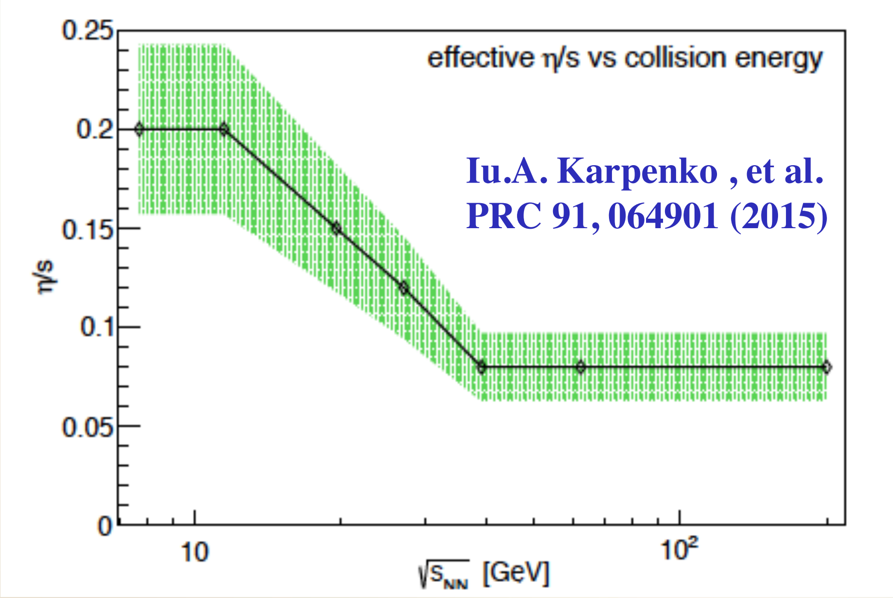

QCD Phase Diagram

➢ Strong interest in the experimental measurements which span a broad (μ_B, T) domain.

❖ Investigate signatures for the first-order phase transition

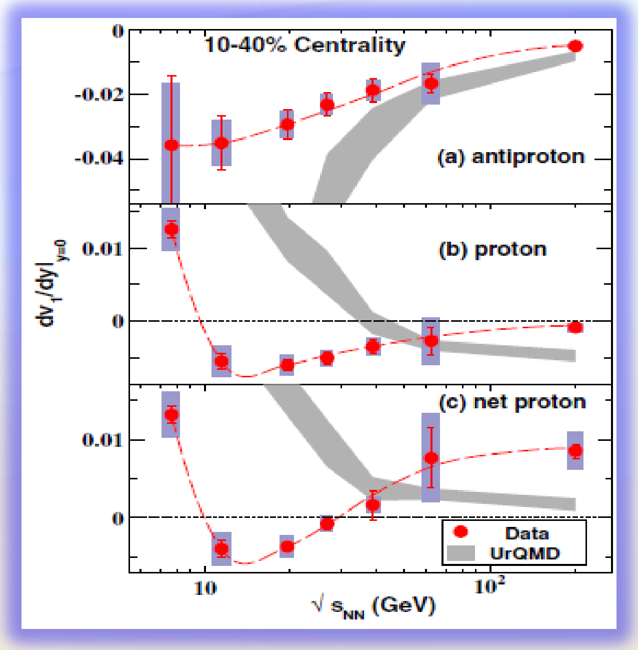

STAR
PRL 112, 162 301 (2014)

QCD Phase Diagram

- Strong interest in the experimental measurements which span a broad (μ_B, T) domain.

- Investigate signatures for the first-order phase transition

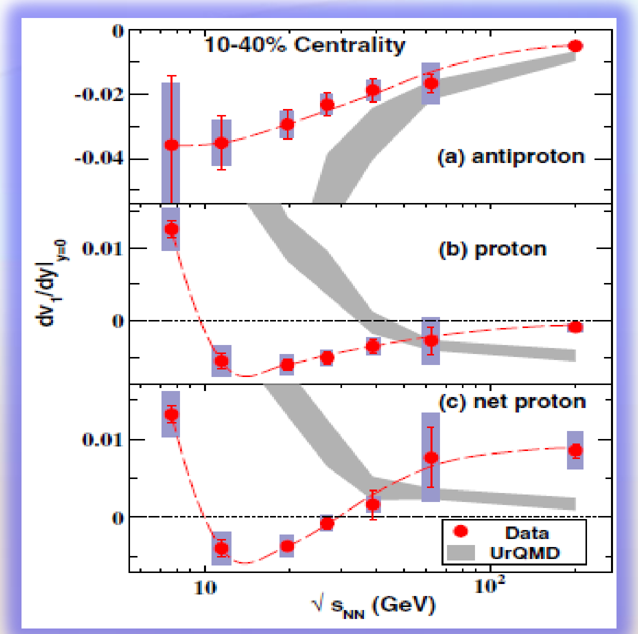

STAR
PRL 112, 162 301 (2014)

- Search for critical fluctuations

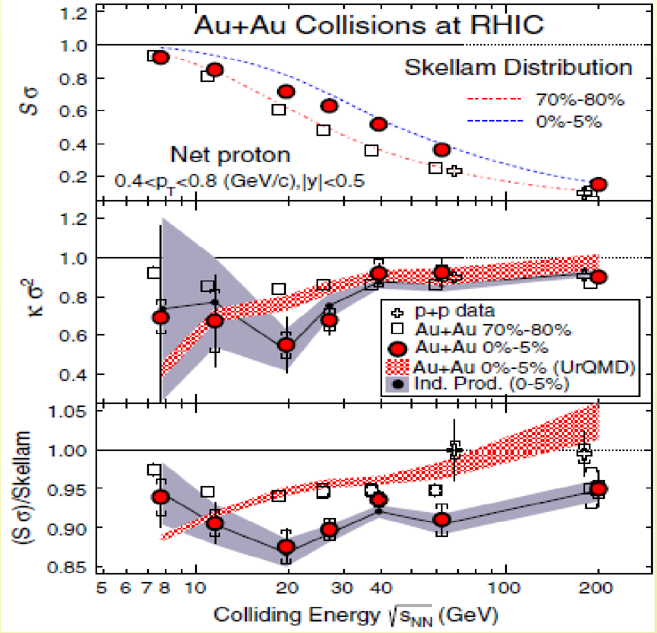

STAR
PRL 112, 032 302 (2014)

Azimuthal anisotropic flow

- Comprehensive set of flow measurements are important to study;
  - ✓ Differentiate between initial-state models
    - Initial-state eccentricity & its fluctuations

Azimuthal anisotropic flow

- Comprehensive set of flow measurements are important to study;
  - ✓ Differentiate between initial-state models
    - ❑ Initial-state eccentricity & its fluctuations
  - ✓ Transport coefficients ($^{\eta}/_{s}$, etc)
    - ❑ Pin down the temperature dependence of the transport coefficients

Azimuthal anisotropic flow

- Comprehensive set of flow measurements are important to study;
  - ✓ Differentiate between initial-state models
    - Initial-state eccentricity & its fluctuations
  - ✓ Transport coefficients ($^{\eta}/_{s}$, etc)
    - Pin down the temperature dependence of the transport coefficients
  - ✓ Detailed flow measurements could aid ongoing efforts to search for the critical end point(CEP)

Azimuthal anisotropic flow

Asymmetry in initial geometry → Final state momentum anisotropy (flow)

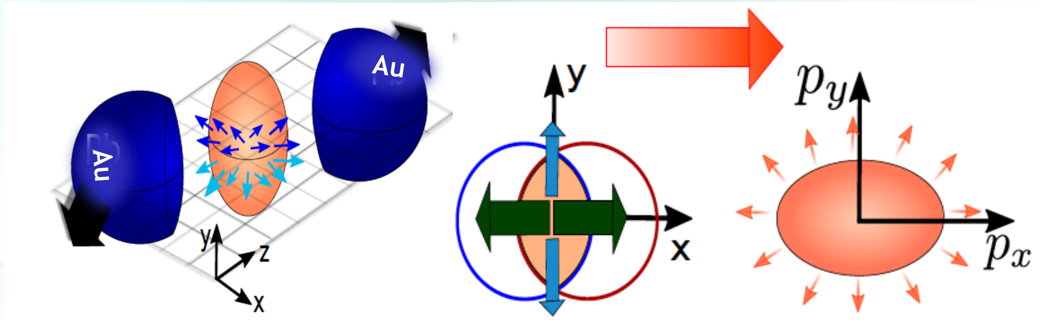

$$^{dN}/_{d\varphi} = 1 + 2\sum_{n}^{\infty} v_n \cos(\varphi - \Psi_n)$$

Dipole asymmetry

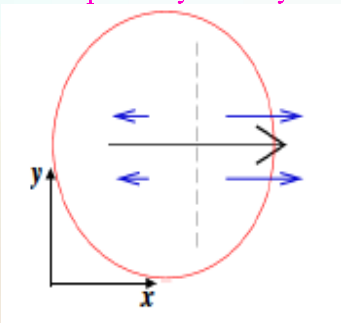

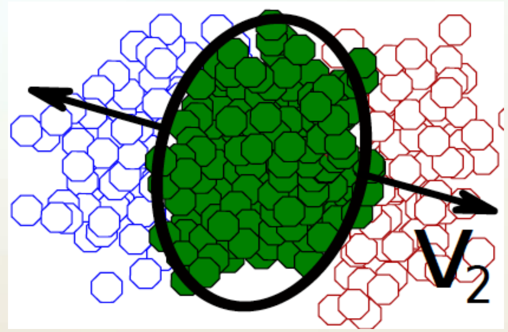

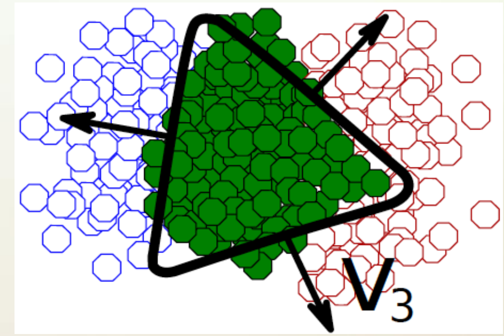

Azimuthal anisotropic flow

Asymmetry in initial geometry → Final state momentum anisotropy (flow)

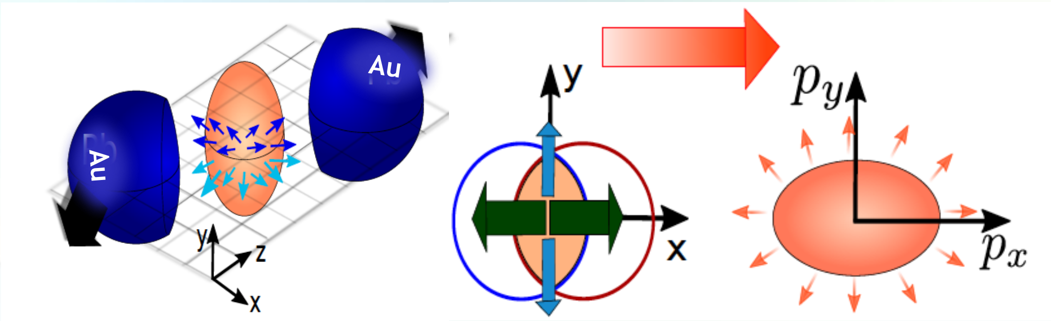

$$ {}^{dN}/_{d\varphi} = 1 + 2 \sum_{n}^{\infty} v_n \cos(\varphi - \Psi_n) $$

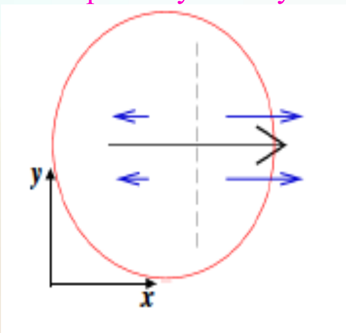

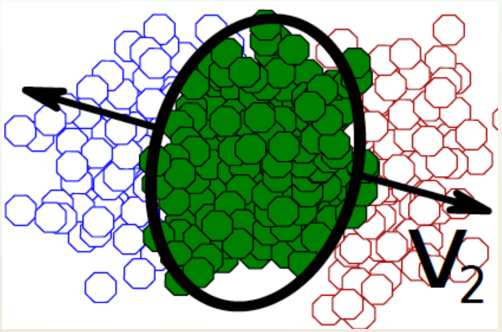

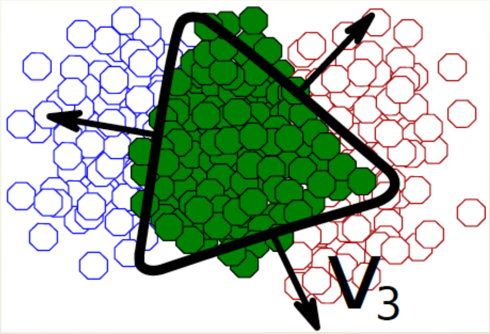

- The flow harmonic coefficients v_n are influenced by eccentricities (ε_n) [and their fluctuations], the speed of sound $c_s(\mu_B, T)$, and transport coefficients $\left(\frac{\eta}{s}, \frac{\zeta}{s}, \ldots\right)$

Datasets

➢ Collected data for Au+Au at different $\sqrt{s_{NN}}$ by STAR detector at RHIC will be presented

STAR Detector at RHIC

➢ TPC detector mainly get used in the current analysis

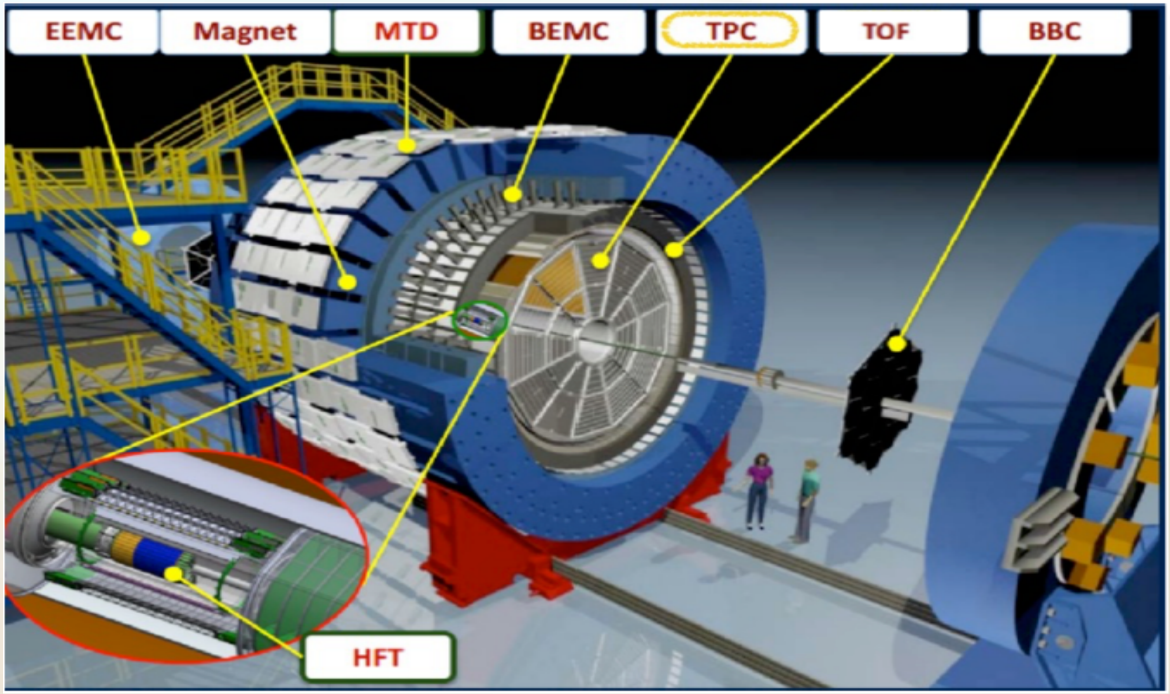

Azimuthal anisotropy measurements

Correlation function

Two-particle correlation function $Cr(\Delta\varphi = \varphi_{\mathrm{a}} - \varphi_b)$,

$$Cr(\Delta\varphi) = dN/d\Delta\varphi \quad \text{and} \quad v_n^{ab} = \frac{\sum_{\Delta\varphi} Cr(\Delta\varphi)\cos(n\,\Delta\varphi)}{\sum_{\Delta\varphi} Cr(\Delta\varphi)}$$

Azimuthal anisotropy measurements

Correlation function

Two-particle correlation function $Cr(\Delta\varphi = \varphi_{\mathrm{a}} - \varphi_b)$,

$$Cr(\Delta\varphi) = dN/d\Delta\varphi \quad \text{and} \quad v_n^{ab} = \frac{\sum_{\Delta\varphi} Cr(\Delta\varphi)\cos(n\,\Delta\varphi)}{\sum_{\Delta\varphi} Cr(\Delta\varphi)}$$

Flow

Non-flow

Azimuthal anisotropy measurements

Correlation function

Two-particle correlation function $Cr(\Delta\varphi = \varphi_a - \varphi_b)$,

$Cr(\Delta\varphi) = dN/d\Delta\varphi$ and $v_n^{ab} = \frac{\sum_{\Delta\varphi} Cr(\Delta\varphi)\cos(n\,\Delta\varphi)}{\sum_{\Delta\varphi} Cr(\Delta\varphi)}$

$n > 1$

$v_n^{ab} = v_n^a v_n^b + \delta_{short}$

Flow

Non-flow

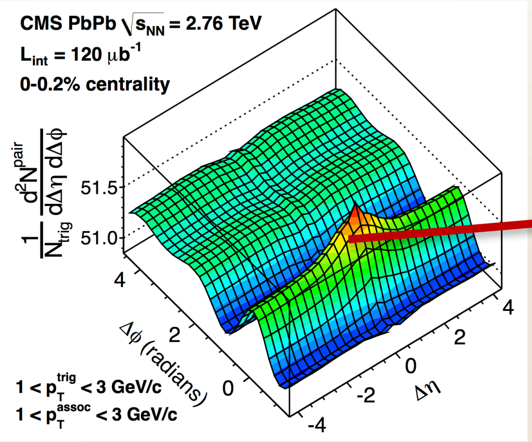

Short − range

HBT

Decay

Charge

Non-flow suppression is needed

Azimuthal anisotropy measurements

Correlation function

Two-particle correlation function $Cr(\Delta\varphi = \varphi_a - \varphi_b)$,

$$Cr(\Delta\varphi) = dN/d\Delta\varphi \quad \text{and} \quad v_n^{ab} = \frac{\sum_{\Delta\varphi} Cr(\Delta\varphi)\cos(n\,\Delta\varphi)}{\sum_{\Delta\varphi} Cr(\Delta\varphi)}$$

$n > 1$

$$v_n^{ab} = v_n^a v_n^b + \delta_{short}$$

$n = 1$

$$v_1^{ab} = v_1^a v_1^b + \delta_{long}$$

Flow

Non-flow

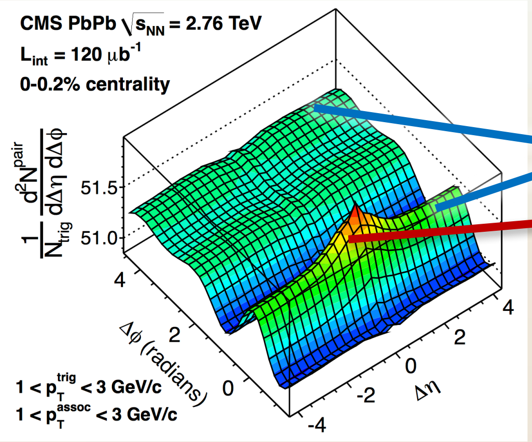

Long – range

Short – range

Momentum Conservation

HBT

Di–jets

Decay

Charge

Non-flow suppression is needed

Short – range Non–flow

HBT

Decay

Short-range non-flow suppression

The v_2 vs centrality at $\sqrt{s_{NN}} = 200$ using different $\Delta\eta$ cuts

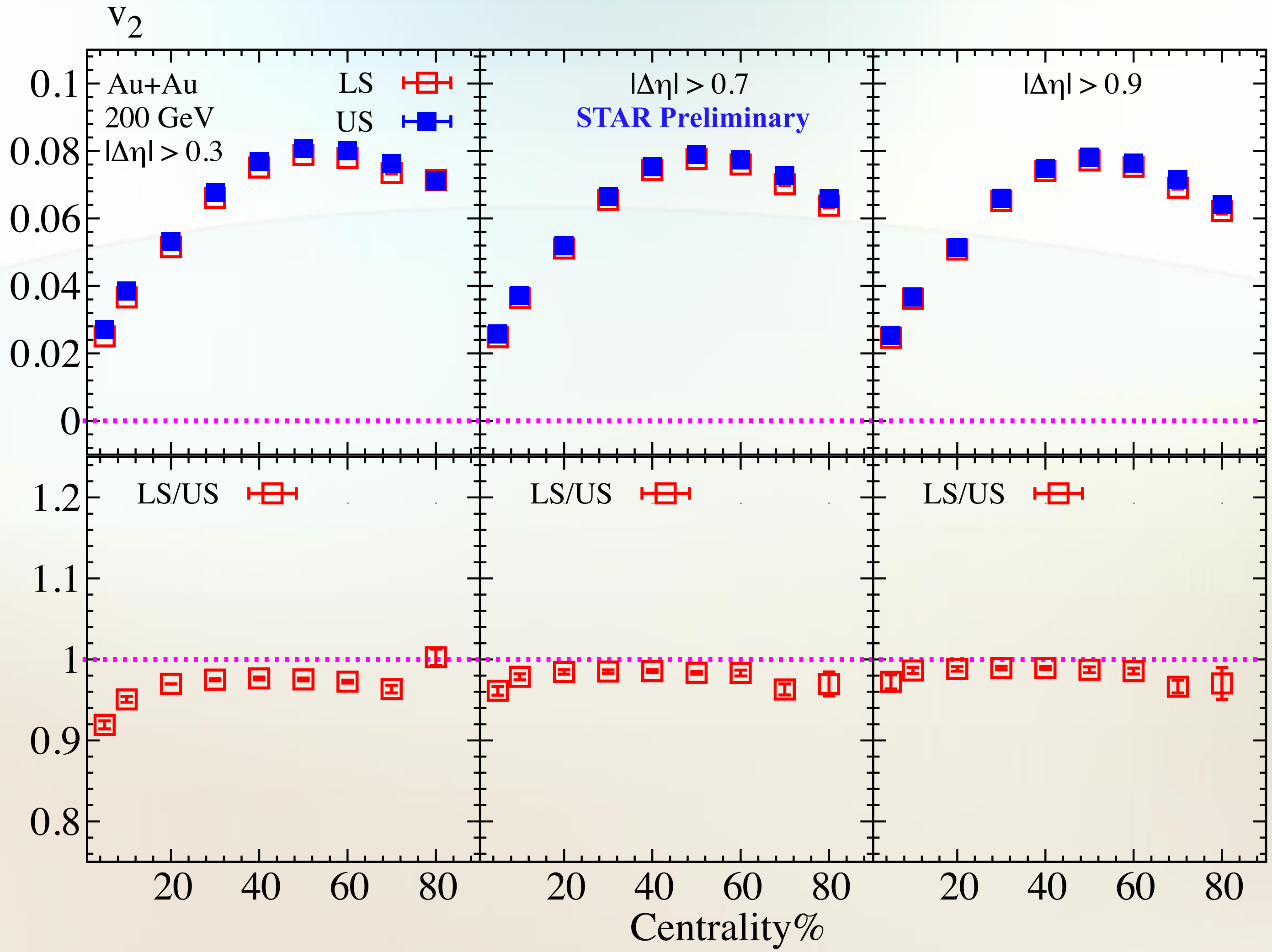

- Short-range non-flow effect get reduced using $|\Delta\eta| > 0.7$ cut

Long – range

Momentum Conservation

Long-range non-flow suppression

arXiv:1203.0931
arXiv:1203.3410
arXiv:1208.1874
arXiv:1208.1887
arXiv:1211.7162

$$v_1^{ab} = v_1^a v_1^b + \delta_{long} \quad n = 1$$

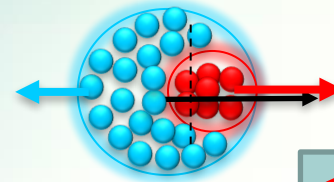

$$v_{11}(p_T^a, p_T^b) = v_1^{even}(p_T^a) v_1^{even}(p_T^b) - C\, p_T^a\, p_T^b \quad \boxed{1}$$

$C \propto (<p_T^2><Mult>)^{-1}$

v_{11} in Eq(1) represents NxM matrix which we fit with N+1 parameters

Long – range

Momentum Conservation

Long-range non-flow suppression

arXiv:1203.0931
arXiv:1203.3410
arXiv:1208.1874
arXiv:1208.1887
arXiv:1211.7162

$$v_1^{ab} = v_1^a v_1^b + \delta_{long} \quad n = 1$$

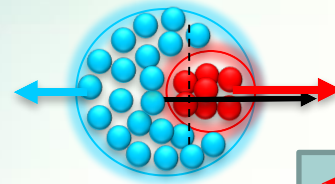

$$v_{11}(p_T^a, p_T^b) = v_1^{even}(p_T^a) v_1^{even}(p_T^b) - C\, p_T^a\, p_T^b \qquad \boxed{1}$$

$$C \propto (< p_T^2 >< Mult >)^{-1}$$

v_{11} in Eq(1) represents NxM matrix which we fit with N+1 parameters

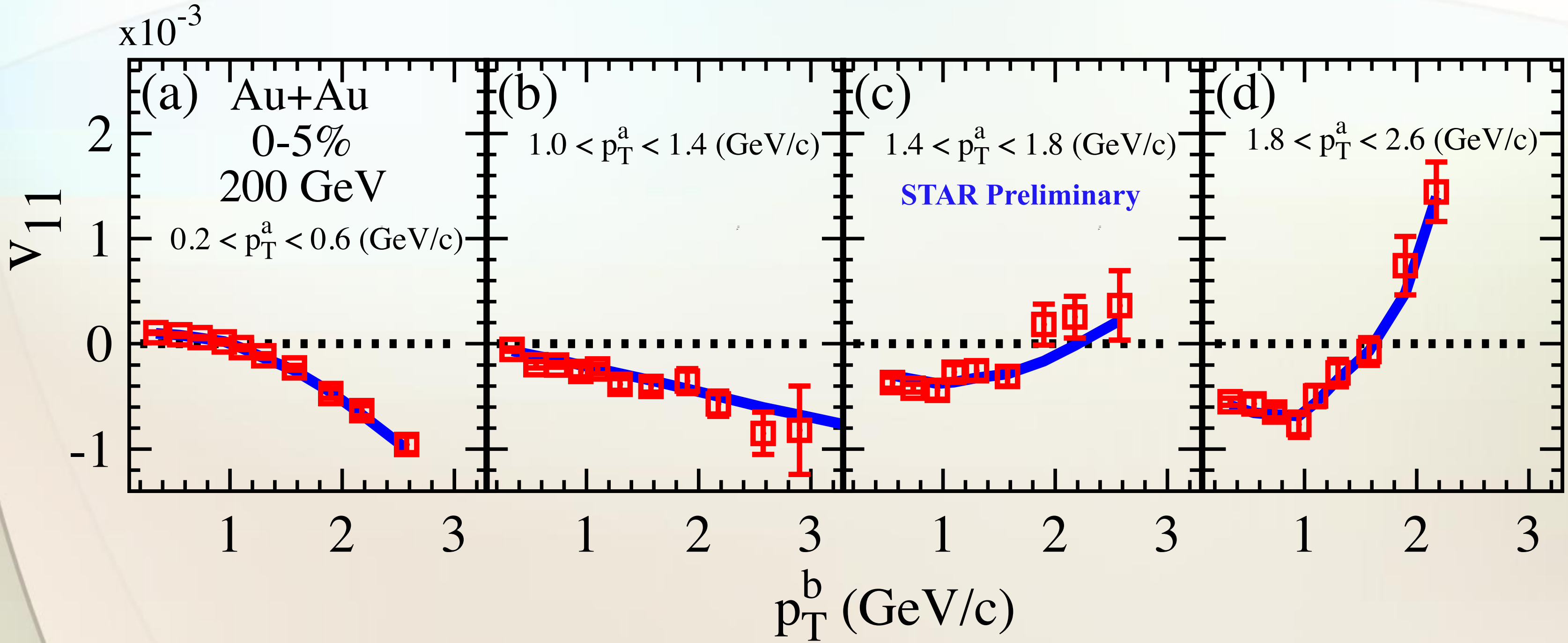

➢ Good simultaneous fit ($\frac{\chi^2}{ndf}$ ~ 1.1) obtained with Eq. 1

Long – range

Momentum Conservation

Long-range non-flow suppression

arXiv:1203.0931
arXiv:1203.3410
arXiv:1208.1874
arXiv:1208.1887
arXiv:1211.7162

$$v_1^{ab} = v_1^a v_1^b + \delta_{long} \quad n = 1$$

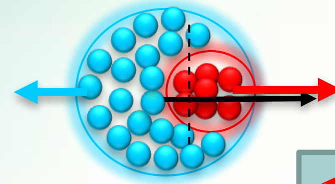

$$v_{11}(p_T^a, p_T^b) = v_1^{even}(p_T^a) v_1^{even}(p_T^b) - C\, p_T^a\, p_T^b \qquad \boxed{1}$$

$C \propto (<p_T^2><Mult>)^{-1}$

v_{11} in Eq(1) represents NxM matrix which we fit with N+1 parameters

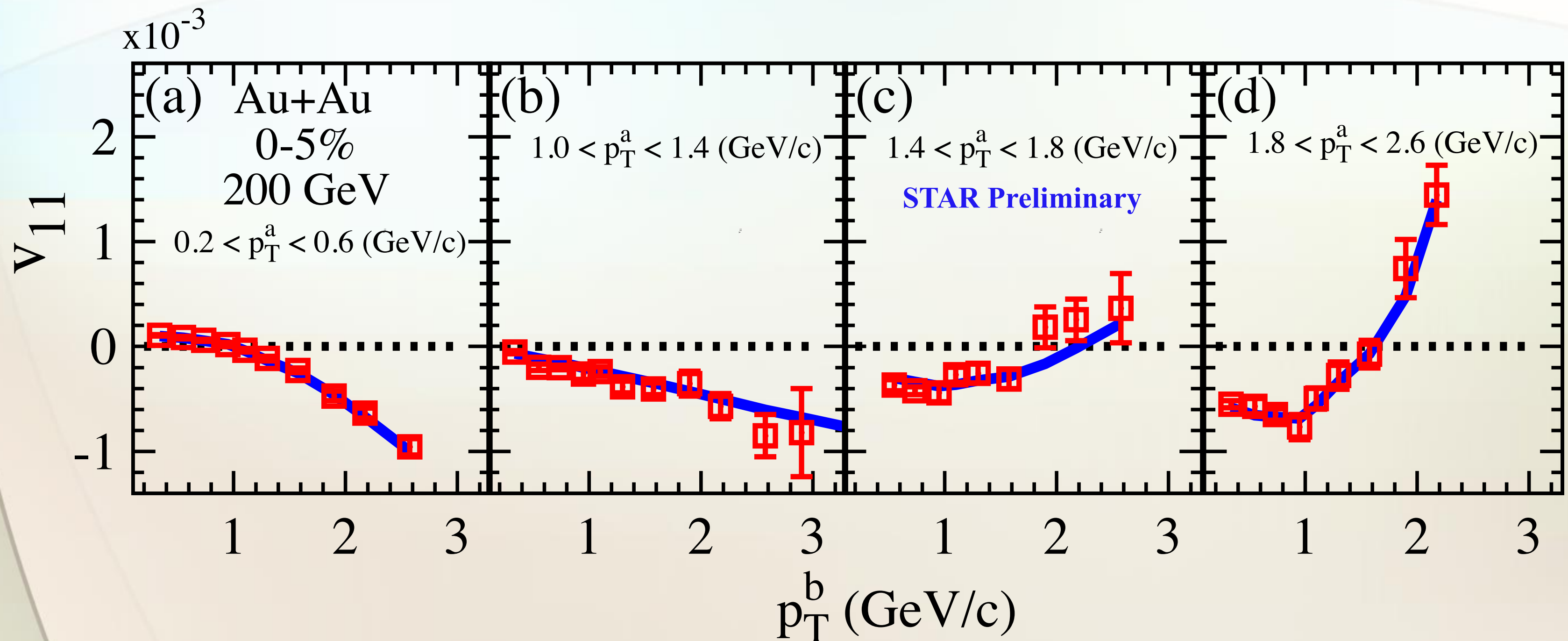

- Good simultaneous fit ($\frac{\chi^2}{ndf} \sim 1.1$) obtained with Eq. 1
- v_{11} characteristic behavior gives a good constraint for $\boldsymbol{v_1^{even}(p_T)}$ extraction

Long − range

Momentum Conservation

$|\eta| < 1$ and $|\Delta\eta| > 0.7$

Long-range non-flow suppression

$$\mathbf{v_{11}}(p_T^a, p_T^b) = v_1^{even}(p_T^a)v_1^{even}(p_T^b) - C\, p_T^a\, p_T^b$$

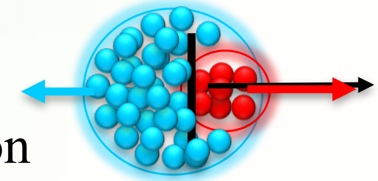

The extracted $v_1^{even}(p_T)$ and the momentum conservation parameter C at $\sqrt{s_{NN}} = 200$

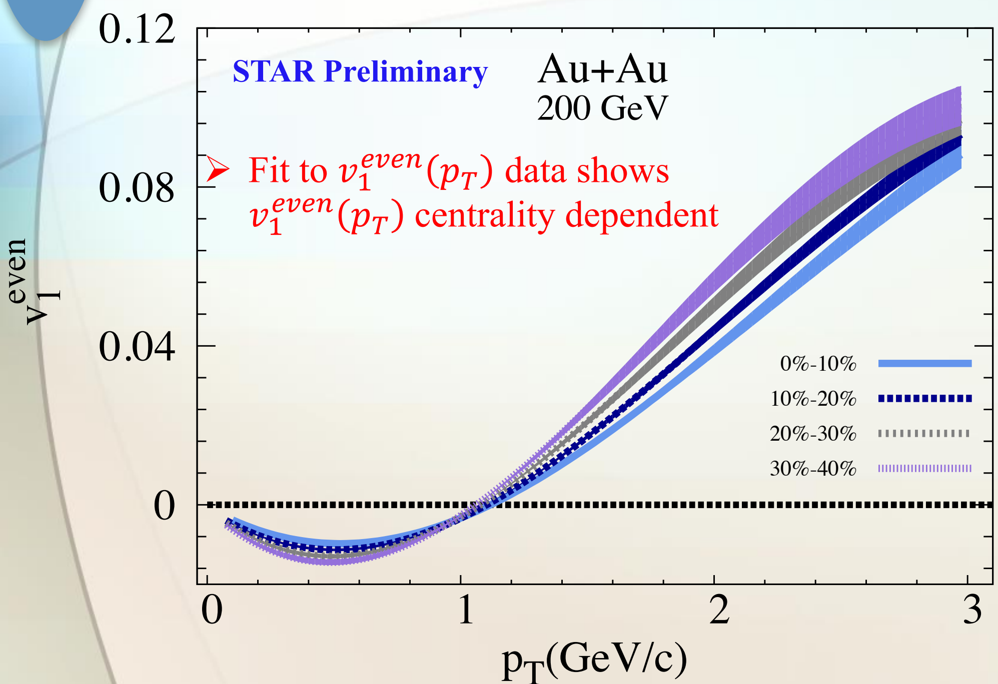

- ➢ The characteristic behavior of $v_1^{even}(p_T)$ shows a weak centrality dependence

$Long - range$

$Momentum\ Conservation$

Long-range non-flow suppression

$|\eta| < 1$ and $|\Delta\eta| > 0.7$

$$\mathbf{v_{11}}(p_T^a, p_T^b) = v_1^{even}(p_T^a)v_1^{even}(p_T^b) - C\, p_T^a\, p_T^b$$

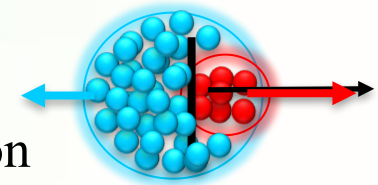

The extracted $v_1^{even}(p_T)$ and the momentum conservation parameter C at $\sqrt{s_{NN}} = 200$

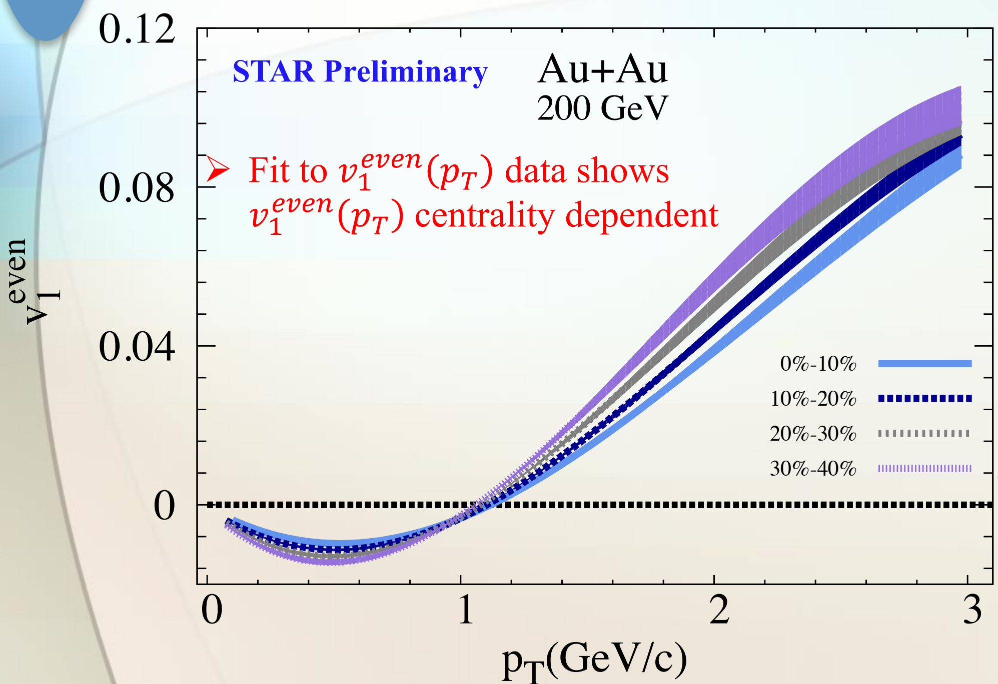

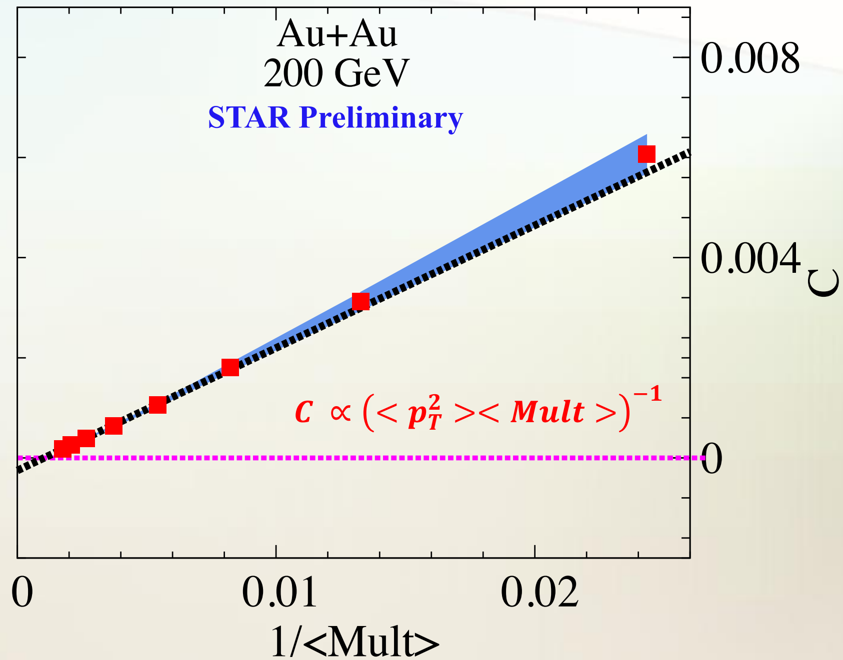

- The characteristic behavior of $v_1^{even}(p_T)$ shows a weak centrality dependence

- The momentum conservation parameter C scales as $< \boldsymbol{Mult} >^{-1}$

Flow harmonics

$\boldsymbol{v}_n(\eta, p_T)$

$\boldsymbol{v}_n(Cent)$

Flow harmonics

$v_n(\eta, p_T)$

$v_n(\sqrt{s_{NN}})$

$v_n(Cent)$

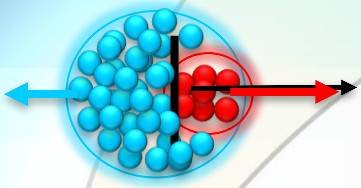

Transverse momentum dependence of v_1^{even}

$$\mathbf{v_{11}}(p_T^a, p_T^t) = v_1^{even}(p_T^a) v_1^{even}(p_T^t) - C\, p_T^a\, p_T^t$$

The extracted $v_1^{even}(p_T)$ at all BES energies

Hydro
E.Retinskaya , et al.
PRL 108, 252302 (2012)

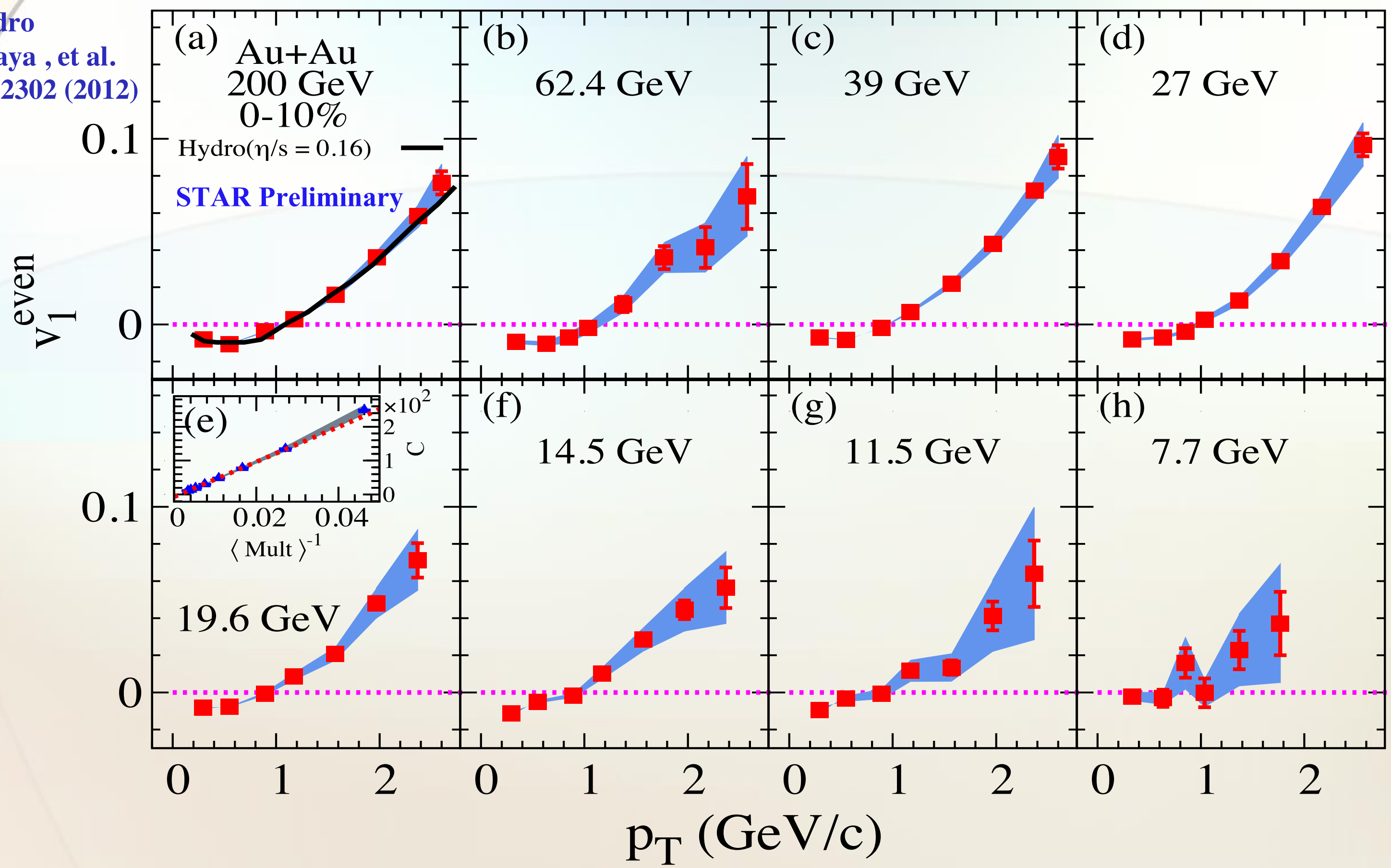

- ➢ Similar characteristic behavior of $v_1^{even}(p_T)$ at all energies
- ➢ $v_1^{even}(p_T)$ agrees with hydrodynamic calculations at 200 GeV
- ➢ Momentum conservation parameter C scales as $\langle Mult \rangle^{-1}$

Centrality dependence dependence of v_1^{even}

$$\mathbf{v_{11}}(p_T^a, p_T^t) = v_1^{even}(p_T^a)v_1^{even}(p_T^t) - C\, p_T^a\, p_T^t$$

The extracted $\boldsymbol{v_1^{even}}(Cent)$ and the momentum conservation parameter at different beam energies

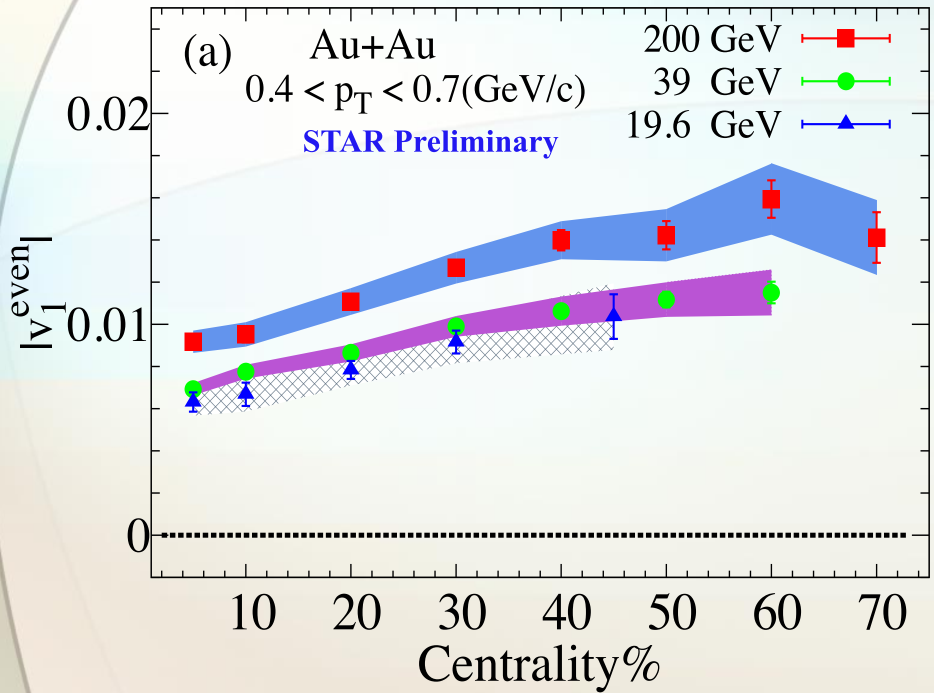

For different beam energies;

- v_1^{even} increases weakly as collisions become more peripheral

Centrality dependence dependence of v_1^{even}

$$\mathbf{v_{11}}(p_T^a, p_T^t) = v_1^{even}(p_T^a)v_1^{even}(p_T^t) - C\, p_T^a\, p_T^t$$

The extracted $\boldsymbol{v_1^{even}}(Cent)$ and the momentum conservation parameter at different beam energies

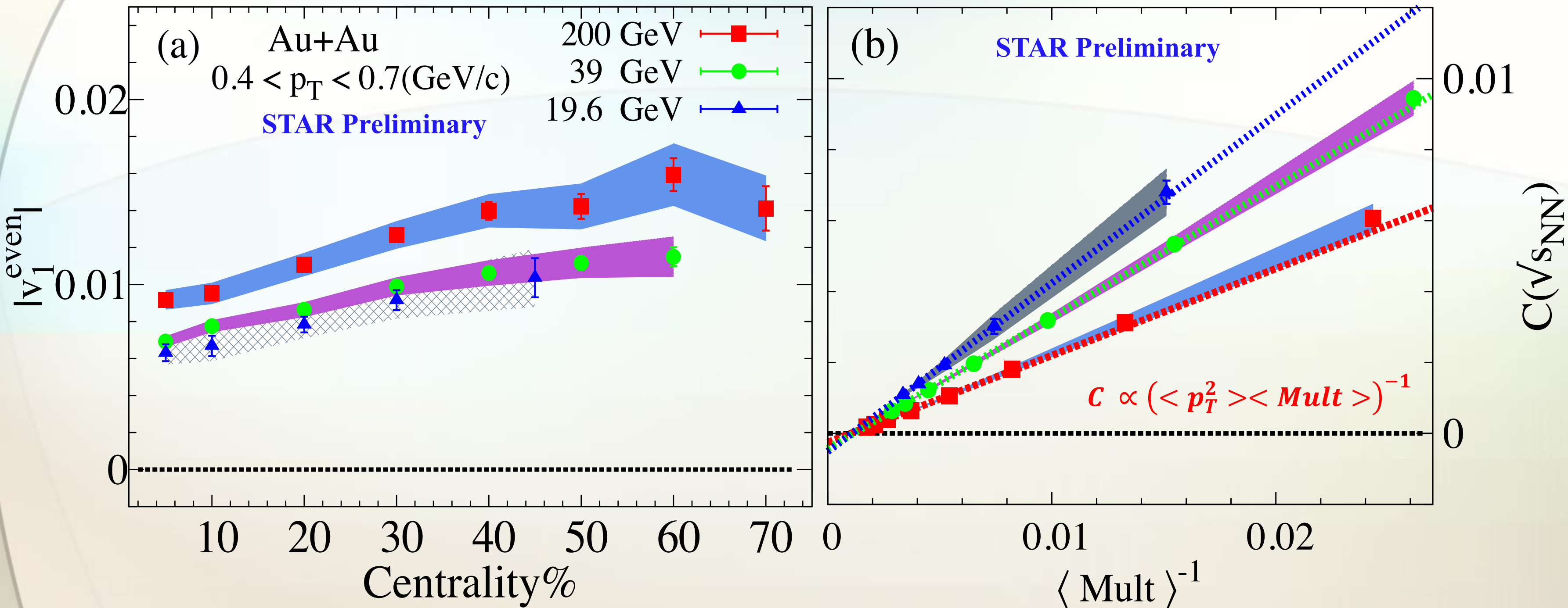

For different beam energies;

- ➢ v_1^{even} increases weakly as collisions become more peripheral
- ➢ Momentum conservation parameter C scales as $\langle Mult \rangle^{-1}$

Pseudorapidity dependence of $v_{n>1}$

$|\eta| < 1$ and $|\Delta\eta| > 0.7$

The extracted $v_{n>1}(\boldsymbol{\eta})$ at all BES energies

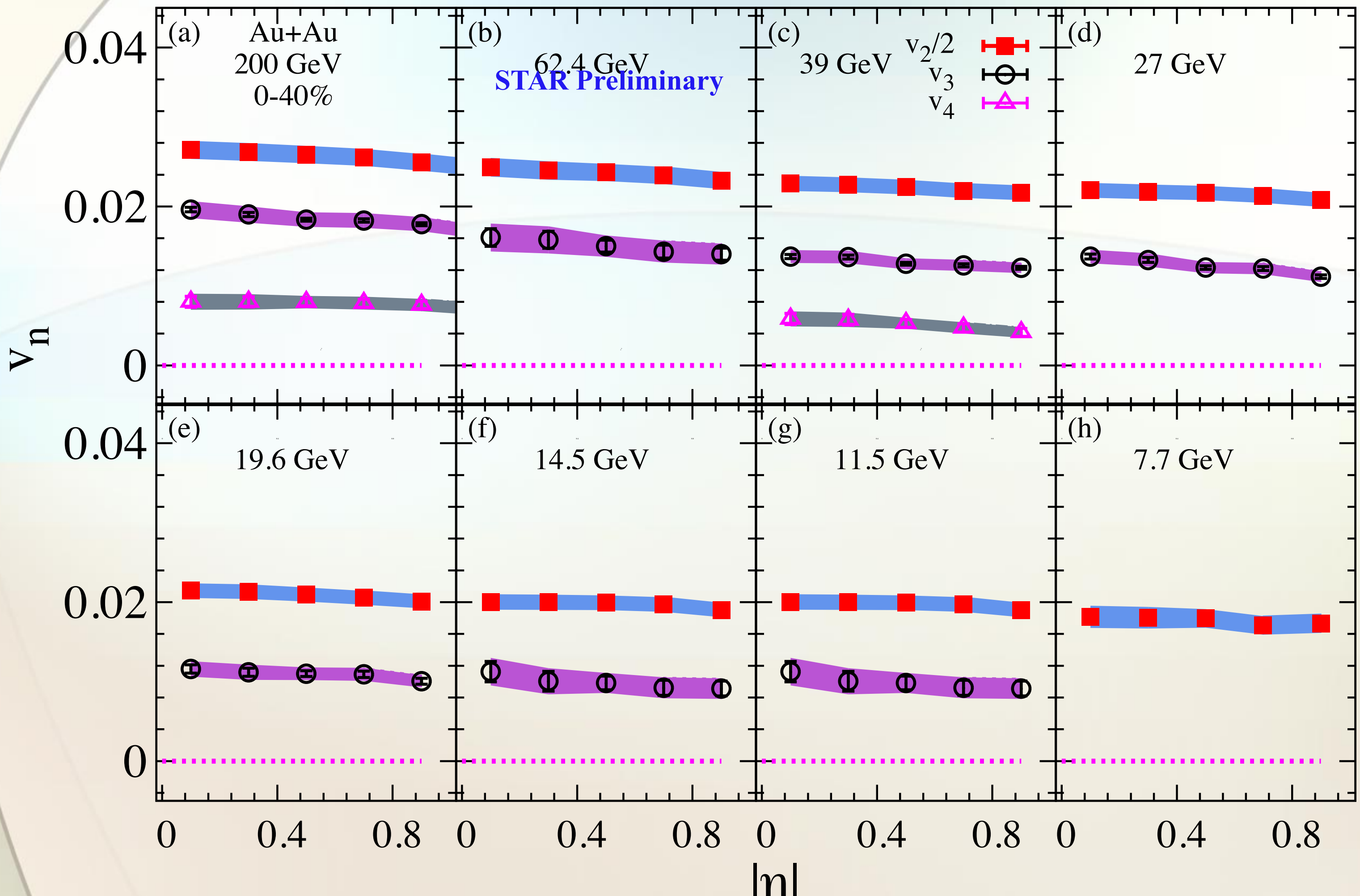

- ➢ $v_n(\boldsymbol{\eta})$ has similar trends for different beam energies.
- ➢ $v_n(\boldsymbol{\eta})$ decreases with harmonic order n.

$|\eta| < 1$ and $|\Delta\eta| > 0.7$

Transverse momentum dependence of $v_{n>1}$

The extracted $v_{n>1}(p_T)$ at all BES energies

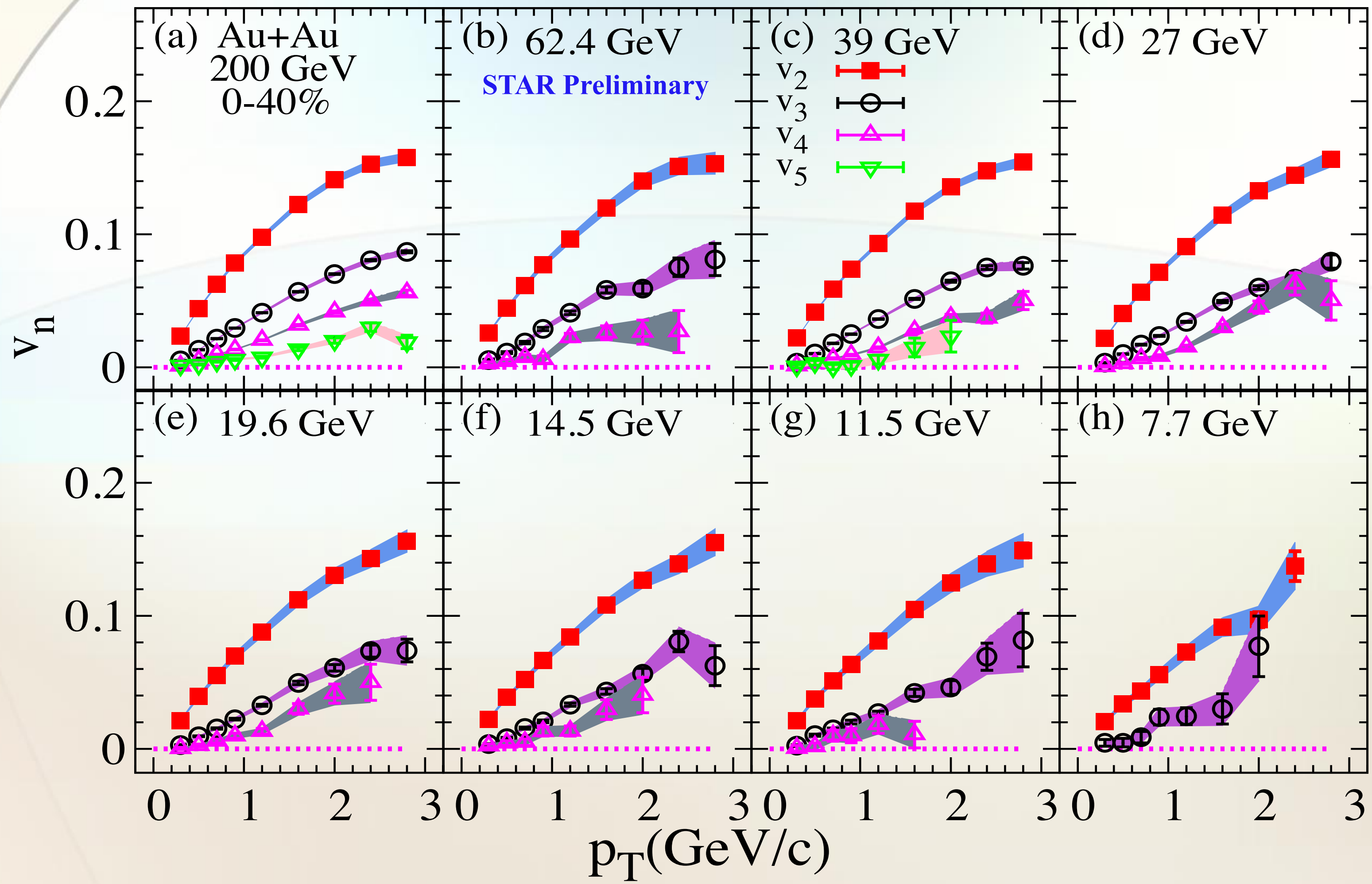

- $v_n(p_T)$ has similar trends for different beam energies.
- $v_n(p_T)$ decreases with harmonic order n.

Centrality dependence of $v_{n>1}$

The extracted $v_{n>1}$(Centrality) at all BES energies

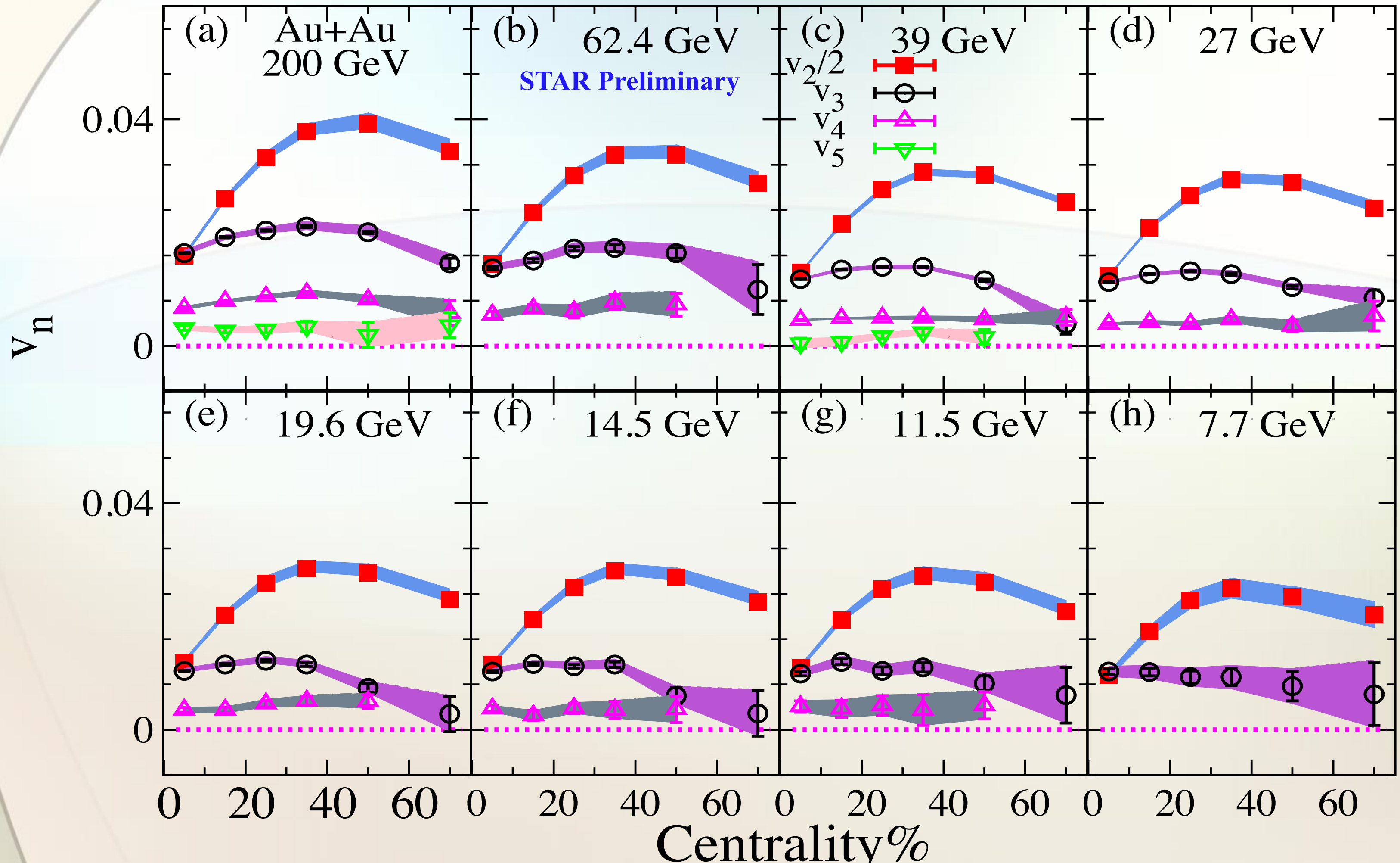

➢ v_n(Centrality) has similar trends for different beam energies.

➢ v_n(Centrality) decreases with harmonic order n.

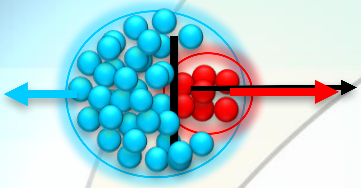

Beam-energy dependence of v_1^{even}

$|\eta| < 1$ and $|\Delta\eta| > 0.7$

$$\mathbf{v_{11}}(\boldsymbol{p_T^a}, \boldsymbol{p_T^t}) = \boldsymbol{v_1^{even}}(\boldsymbol{p_T^a})\boldsymbol{v_1^{even}}(\boldsymbol{p_T^t}) - \boldsymbol{C}\,\boldsymbol{p_T^a}\,\boldsymbol{p_T^t}$$

The extracted $\boldsymbol{v_1^{even}}$ vs $\sqrt{s_{NN}}$ at 0%-10% centrality

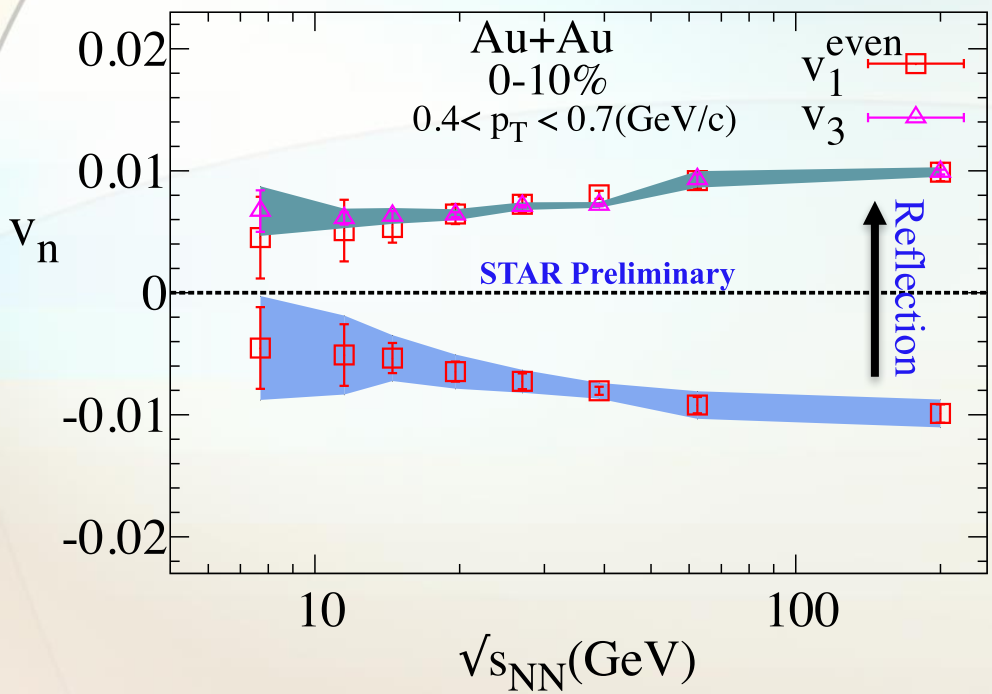

➢ $|v_1^{even}|$ shows similar values to v_3 at $0.4 < p_T < 0.7(GeV/c)$

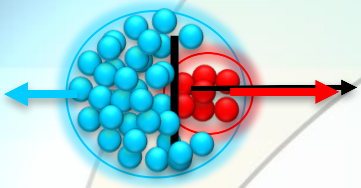

Beam-energy dependence of v_1^{even}

$|\eta| < 1$ and $|\Delta\eta| > 0.7$

$$\mathbf{v_{11}(p_T^a, p_T^t) = v_1^{even}(p_T^a) v_1^{even}(p_T^t) - C\, p_T^a\, p_T^t}$$

The extracted $\boldsymbol{v_1^{even}}$ vs $\sqrt{s_{NN}}$ at 0%-10% centrality

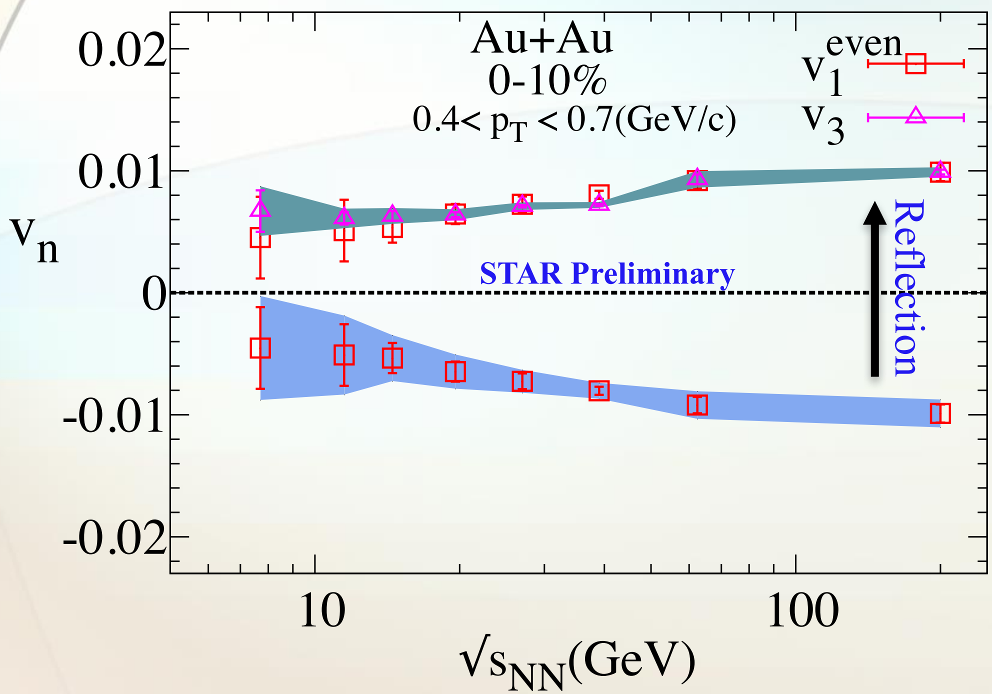

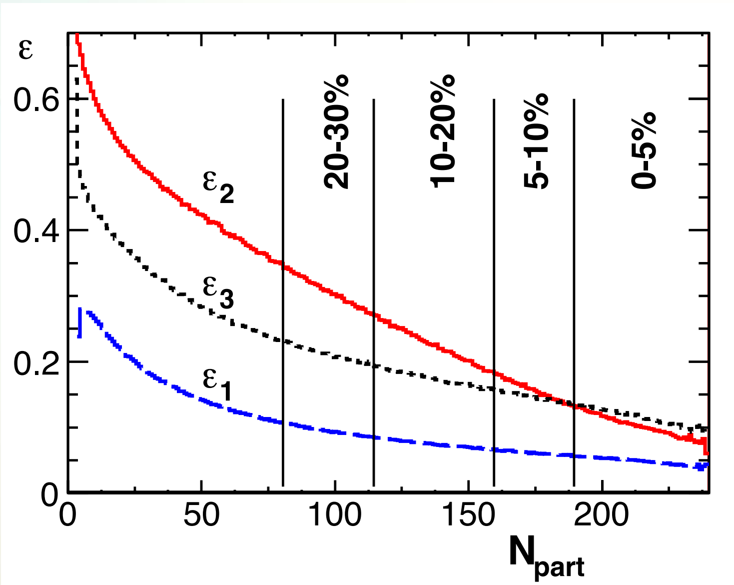

P.Bożek
PLB 717, 287-290 (2012)

- $|v_1^{even}|$ shows similar values to v_3 at $0.4 < p_T < 0.7(GeV/c)$
- $\varepsilon_3 > \varepsilon_1$
  - ✓ v_3 has larger viscous damping effect than v_1^{even}

Beam-energy dependence of $v_{n>1}$

The extracted $v_{n>1}$ vs $\sqrt{s_{NN}}$ at 0-40% centrality

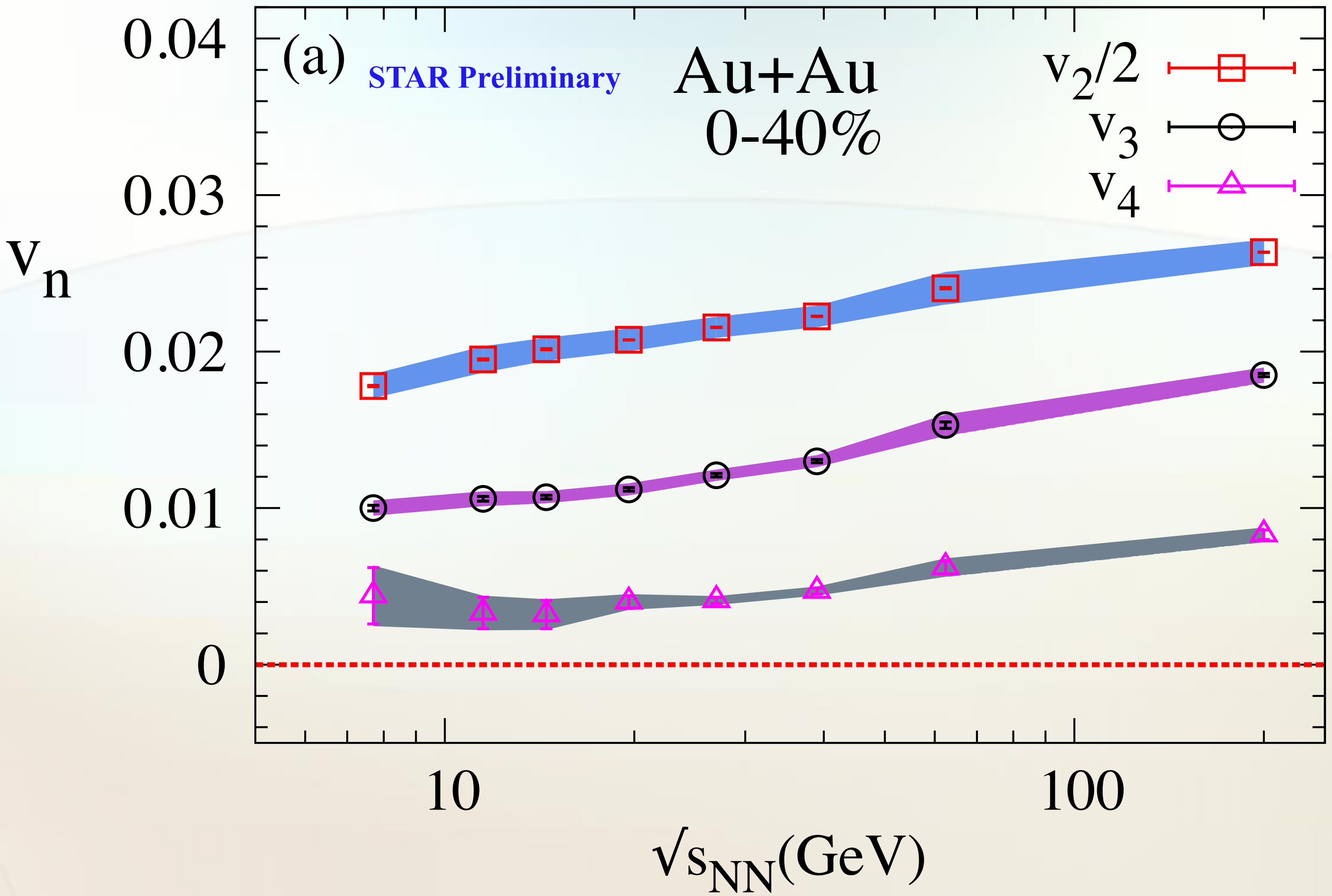

- $v_n(\sqrt{s_{NN}})$ shows a monotonic increase with beam-energy.
- $v_n(\sqrt{s_{NN}})$ decreases with harmonic order n (viscous effects).

Summary-I

Comprehensive set of flow measurements were studied for Au+Au collision system at all BES energies with one set of cuts.

- For $n > 1$;
  - ✓ v_n decreases with harmonic order n.
- For $n = 1$;

Summary-I

Comprehensive set of flow measurements were studied for Au+Au collision system at all BES energies with one set of cuts.

- For $n > 1$;
  - ✓ v_n decreases with harmonic order n.
  - ✓ $v_n(p_T,\ \eta,$ Centrality) indicates a similar trend for different beam energies.

- For $n = 1$;

Summary-I

Comprehensive set of flow measurements were studied for Au+Au collision system at all BES energies with one set of cuts.

- For $\mathrm{n} > 1$;
  - ✓ v_n decreases with harmonic order n.
  - ✓ $v_n(p_T,\ \eta,$ Centrality) indicates a similar trend for different beam energies.
  - ✓ $v_n\left(\sqrt{s_{NN}}\right)$ shows a monotonic increase with beam-energy.
- For $\mathrm{n} = 1$;

Summary-I

Comprehensive set of flow measurements were studied for Au+Au collision system at all BES energies with one set of cuts.

- For $\mathrm{n} > 1$;
  - ✓ v_n decreases with harmonic order n.
  - ✓ $v_n(p_T,\ \eta,$ Centrality) indicates a similar trend for different beam energies.
  - ✓ $v_n\left(\sqrt{s_{NN}}\right)$ shows a monotonic increase with beam-energy.
- For $\mathrm{n} = 1$;
  - ✓ Similar characteristic behavior of $v_1^{even}(p_T)$ at all energies.

Summary-I

Comprehensive set of flow measurements were studied for Au+Au collision system at all BES energies with one set of cuts.

- For $\mathrm{n} > 1$;
  - ✓ v_n decreases with harmonic order n.
  - ✓ $v_n(p_T,\ \eta,$ Centrality) indicates a similar trend for different beam energies.
  - ✓ $v_n\left(\sqrt{s_{NN}}\right)$ shows a monotonic increase with beam-energy.
- For $\mathrm{n} = 1$;
  - ✓ Similar characteristic behavior of $v_1^{even}(p_T)$ at all energies.
  - ✓ Momentum conservation parameter C scales as $\langle Mult \rangle^{-1}$

Summary-I

Comprehensive set of flow measurements were studied for Au+Au collision system at all BES energies with one set of cuts.

- For $\mathrm{n} > 1$;
  - ✓ v_n decreases with harmonic order n.
  - ✓ $v_n(p_T,\ \eta,$ Centrality) indicates a similar trend for different beam energies.
  - ✓ $v_n\left(\sqrt{s_{NN}}\right)$ shows a monotonic increase with beam-energy.
- For $\mathrm{n} = 1$;
  - ✓ Similar characteristic behavior of $v_1^{even}(p_T)$ at all energies.
  - ✓ Momentum conservation parameter C scales as $\langle Mult \rangle^{-1}$
  - ✓ $|v_1^{even}|$ shows similar values to v_3 (larger viscous effect for v_3)

Summary-I

Comprehensive set of flow measurements were studied for Au+Au collision system at all BES energies with one set of cuts.

- For $n > 1$;
  - ✓ v_n decreases with harmonic order n.
  - ✓ $v_n(p_T,\ \eta,$ Centrality) indicates a similar trend for different beam energies.
  - ✓ $v_n\left(\sqrt{s_{NN}}\right)$ shows a monotonic increase with beam-energy.
- For $n = 1$;
  - ✓ Similar characteristic behavior of $v_1^{even}(p_T)$ at all energies.
  - ✓ Momentum conservation parameter C scales as $\langle Mult\rangle^{-1}$
  - ✓ $|v_1^{even}|$ shows similar values to v_3 (larger viscous effect for v_3)
- More information could be extracted from v_n measurements via the acoustic ansatz

Acoustic ansatz

PRC 84, 034908 (2011) P. Staig and E. Shuryak.	arXiv:1305.3341 Roy A. Lacey, et al.
PRC 88, 044915 (2013) E. Shuryak and I. Zahed	arXiv:1601.06001 Roy A. Lacey, et al.

- v_n measurements are sensitive to system shape (ε_n), size (RT) and transport coefficients $\left(\frac{\eta}{s}, \frac{\zeta}{s}, \ldots\right)$.

Acoustic ansatz

PRC 84, 034908 (2011)
P. Staig and E. Shuryak.

PRC 88, 044915 (2013)
E. Shuryak and I. Zahed

arXiv:1305.3341
Roy A. Lacey, et al.

arXiv:1601.06001
Roy A. Lacey, et al.

- v_n measurements are sensitive to system shape (ε_n), size (RT) and transport coefficients $\left(\frac{\eta}{s}, \frac{\zeta}{s}, \ldots\right)$.
- Acoustic ansatz
  - ✓ Sound attenuation in the viscous matter reduces the magnitude of v_n.

Acoustic ansatz

PRC 84, 034908 (2011) P. Staig and E. Shuryak.	arXiv:1305.3341 Roy A. Lacey, et al.
PRC 88, 044915 (2013) E. Shuryak and I. Zahed	arXiv:1601.06001 Roy A. Lacey, et al.

- v_n measurements are sensitive to system shape (ε_n), size (RT) and transport coefficients $\left(\frac{\eta}{s}, \frac{\zeta}{s}, \ldots\right)$.
- Acoustic ansatz
  - ✓ Sound attenuation in the viscous matter reduces the magnitude of v_n.
- Anisotropic flow attenuation,

$$\frac{v_n}{\varepsilon_n} \propto e^{-\beta n^2}, \; \beta \propto \frac{\eta}{s}\frac{1}{R\,T}$$

i

- From macroscopic entropy considerations

$$S \sim (RT)^3 \sim \langle N_{Ch} \rangle \text{ then } RT \sim \langle N_{Ch} \rangle^{\frac{1}{3}}$$

PRC 84, 034908 (2011)
P. Staig and E. Shuryak.

PRC 88, 044915 (2013)
E. Shuryak and I. Zahed

arXiv:1305.3341
Roy A. Lacey, et al.

arXiv:1601.06001
Roy A. Lacey, et al.

Acoustic ansatz

- v_n measurements are sensitive to system shape (ε_n), size (RT) and transport coefficients $\left(\frac{\eta}{s}, \frac{\zeta}{s}, \dots\right)$.
- Acoustic ansatz
  - ✓ Sound attenuation in the viscous matter reduces the magnitude of v_n.
- Anisotropic flow attenuation,

$$\frac{v_n}{\varepsilon_n} \propto e^{-\beta\, n^2}, \ \beta \propto \frac{\eta}{s}\frac{1}{R\,T} \qquad \boxed{\text{i}}$$

- From macroscopic entropy considerations

$$S \sim (RT)^3 \sim \langle N_{Ch}\rangle \text{ then } RT \sim \langle N_{Ch}\rangle^{\frac{1}{3}}$$

- We can rewrite Eq(i)

$$\boldsymbol{ln}\left(\frac{v_n}{\varepsilon_n}\right) \propto -\boldsymbol{n}^2(\boldsymbol{\beta}')\langle \boldsymbol{N}_{Ch}\rangle^{-\frac{1}{3}} \quad \text{where} \quad \boldsymbol{\beta}' \propto \frac{\boldsymbol{\eta}}{\boldsymbol{s}}$$

- At the same centrality we have

$$\boldsymbol{ln}\left(\frac{v_n^{1/n}}{v_2^{1/2}}\right) \propto -(\boldsymbol{n}-2)\,(\boldsymbol{\beta}')\langle \boldsymbol{N}_{Ch}\rangle^{-\frac{1}{3}} \quad \text{where} \quad \boldsymbol{\beta}' = \boldsymbol{A}\,\frac{\boldsymbol{\eta}}{\boldsymbol{s}}$$

where A is constant

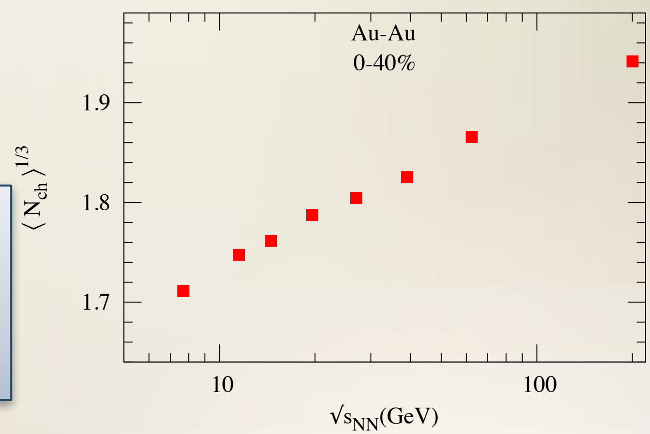

Acoustic ansatz

PRC 84, 034908 (2011)
P. Staig and E. Shuryak.

PRC 88, 044915 (2013)
E. Shuryak and I. Zahed

arXiv:1305.3341
Roy A. Lacey, et al.

arXiv:1601.06001
Roy A. Lacey, et al.

- v_n measurements are sensitive to system shape (ε_n), size (RT) and transport coefficients $\left(\frac{\eta}{s}, \frac{\zeta}{s}, \ldots\right)$.
- Acoustic ansatz
  - ✓ Sound attenuation in the viscous matter reduces the magnitude of v_n.
- Anisotropic flow attenuation,

$$\frac{v_n}{\varepsilon_n} \propto e^{-\beta\, n^2}, \ \beta \propto \frac{\eta}{s} \frac{1}{R\,T} \quad \text{(i)}$$

- From macroscopic entropy considerations

$$S \sim (RT)^3 \sim \langle N_{Ch} \rangle \text{ then } RT \sim \langle N_{Ch} \rangle^{\frac{1}{3}}$$

- We can rewrite Eq(i)

$$\boldsymbol{ln}\left(\frac{v_n}{\varepsilon_n}\right) \propto -n^2 (\beta') \langle N_{Ch} \rangle^{-\frac{1}{3}} \quad \text{where} \quad \beta' \propto \frac{\eta}{s}$$

- At the same centrality we have

$$\boldsymbol{ln}\left(\frac{v_n^{1/n}}{v_2^{1/2}}\right) \propto -(n-2)\, (\beta') \langle N_{Ch} \rangle^{-\frac{1}{3}} \quad \text{where} \quad \beta' = A\, \frac{\eta}{s}$$

where A is constant

$$\boldsymbol{ln}\left(\frac{v_n^{1/n}}{v_2^{1/2}}\right) \langle N_{Ch} \rangle^{\frac{1}{3}} (n-2)^{-1} = \beta''$$

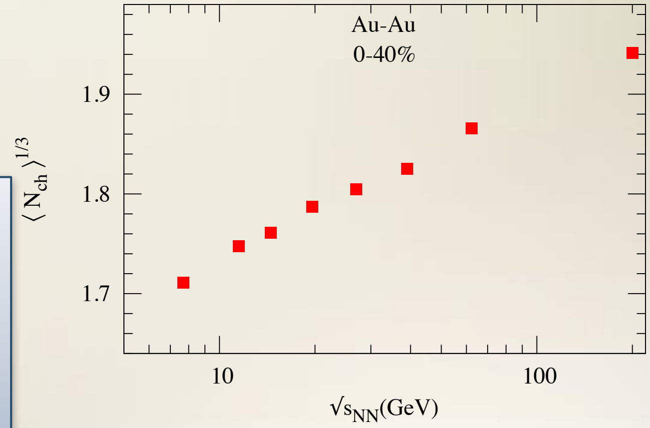

Viscous coefficient

$$\beta'' = \ln\left(\frac{v_n^{1/n}}{v_2^{1/2}}\right) \langle N_{Ch}\rangle^{\frac{1}{3}} \ (n-2)^{-1} = A\frac{\eta}{s}$$

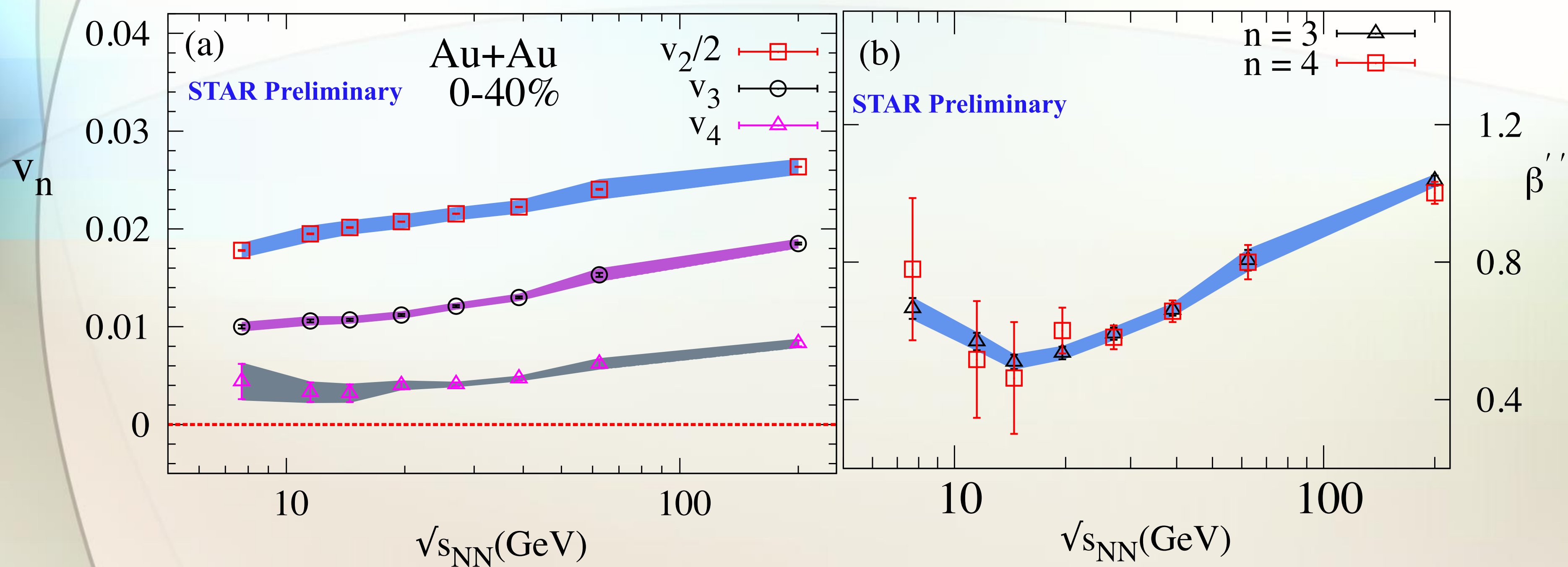

➢ The viscous coefficient shows a non-monotonic behavior with beam-energy

Conclusion

Comprehensive set of STAR measurements presented for $v_n(p_T,\ \eta,\ \text{Centrality}\ and\ \sqrt{s_{NN}})$ for Au+Au collisions.

- For v_n:
  - ✓ $v_n(p_T,\ \eta,\ \text{Centrality})$ indicates a similar trend for different beam energies.

Conclusion

Comprehensive set of STAR measurements presented for $v_n(p_T,\ \eta,$ Centrality $and\ \sqrt{s_{NN}})$ for Au+Au collisions.

- For v_n:
  - ✓ $v_n(p_T,\ \eta,$ Centrality) indicates a similar trend for different beam energies.
  - ✓ Momentum conservation parameter C scales as $\langle Mult \rangle^{-1}$

Conclusion

Comprehensive set of STAR measurements presented for $v_n(p_T,\ \eta,$ Centrality and $\sqrt{s_{NN}})$ for Au+Au collisions.

- For v_n:
  - ✓ $v_n(p_T,\ \eta,$ Centrality) indicates a similar trend for different beam energies.
  - ✓ Momentum conservation parameter C scales as $\langle Mult \rangle^{-1}$
  - ✓ $v_n(\sqrt{s_{NN}})$ shows a monotonic increase with beam-energy.

Conclusion

Comprehensive set of STAR measurements presented for $v_n(p_T,\ \eta,\ \text{Centrality}\ and\ \sqrt{s_{NN}})$ for Au+Au collisions.

- For v_n:
  - ✓ $v_n(p_T,\ \eta,\ \text{Centrality})$ indicates a similar trend for different beam energies.
  - ✓ Momentum conservation parameter C scales as $\langle Mult \rangle^{-1}$
  - ✓ $v_n\left(\sqrt{s_{NN}}\right)$ shows a monotonic increase with beam-energy.
  - ✓ $|v_1^{even}|$ shows similar values to v_3 (larger viscous effect for v_3)

Conclusion

Comprehensive set of STAR measurements presented for $v_n(p_T,\ \eta,$ Centrality $and\ \sqrt{s_{NN}})$ for Au+Au collisions.

- For v_n:
  - ✓ $v_n(p_T,\ \eta,$ Centrality) indicates a similar trend for different beam energies.
  - ✓ Momentum conservation parameter C scales as $\langle Mult \rangle^{-1}$
  - ✓ $v_n(\sqrt{s_{NN}})$ shows a monotonic increase with beam-energy.
  - ✓ $|v_1^{even}|$ shows similar values to v_3 (larger viscous effect for v_3)

The viscous coefficient ($A\frac{\eta}{s}$), is non-monotonic versus the collision-energy with an apparent minimum near ~15 GeV.

THANK YOU